

Direction controllable linearly polarized laser from a dye-doped cholesteric liquid crystal

Ying Zhou, Yuhua Huang, Tsung-Hsien Lin, Liang-Pin Chen,
Qi Hong, and Shin-Tson Wu

College of Optics and Photonics, University of Central Florida, FL 32826
swu@creol.ucf.edu

<http://lcd.creol.ucf.edu>

Abstract: We demonstrate a direction controllable linearly polarized laser from a dye-doped cholesteric liquid crystal (CLC) in a homogeneous cell coated with a metallic mirror on the inner side of a glass substrate. Due to coherent superposition of two orthogonal polarization states, the output laser light becomes linearly polarized and its output energy is greatly enhanced. Moreover, the linear polarization direction angle is proportional to the product of the CLC effective birefringence and cell gap. Hence direction tunable laser devices can be demonstrated by controlling the cell gap and the operating temperature.

©2006 Optical Society of America

OCIS codes: (230.3720) Liquid crystal devices; (160, 3710) Materials

References and links

1. V. I. Kopp, Z. Q. Zhang, and A. Z. Genack, "Lasing in chiral photonic structures," *Prog. Quantum Electron.* **27**, 369-416 (2003).
2. S. T. Wu and D. K. Yang, *Reflective Liquid Crystal Displays*, (Wiley, New York, 2001).
3. J. P. Dowling, M. Scalora, M. J. Bloemer, and C. M. Bowden, "The photonic band edge laser: A new approach to gain enhancement," *J. Appl. Phys.* **75**, 1896-1899 (1994).
4. V. I. Kopp, B. Fan, H. K. M. Vithana, and A. Z. Genack, "Low-threshold lasing at the edge of a photonic stop band in cholesteric liquid crystals," *Opt. Lett.* **23**, 1707-1709 (1998).
5. S. Y. Lin, J. G. Fleming, and I. E. Kady, "Experimental observation of photonic-crystal emission near a photonic band edge," *Appl. Phys. Lett.* **83**, 593-595 (2003).
6. M. Ozaki, M. Kasano, D. Ganzke, W. Haase, and K. Yoshino, "Mirrorless lasing in a dye-doped ferroelectric liquid crystal," *Adv. Mater.* **14**, 306-309 (2002).
7. W. Y. Cao, A. Munoz, P. Palffy-Muhoray, and B. Taheri, "Lasing in a three-dimensional photonic crystal of the liquid crystal blue phase," *Nat. Mater.* **1**, 111-113 (2002).
8. T. Matsui, R. Ozaki, K. Funamoto, M. Ozaki, and K. Yoshino, "Flexible mirrorless laser based on a free-standing film of photo polymerized cholesteric liquid crystal," *Appl. Phys. Lett.* **81**, 3741-3743 (2002).
9. H. Finkelmann, S. T. Kim, A. Munoz, P. Palffy-Muhoray, and B. Taheri, "Tunable mirrorless lasing in cholesteric liquid crystalline elastomers," *Adv. Mater.* **13**, 1069-1072 (2001).
10. S. Furumi, S. Yokoyama, A. Otomo, and S. Mashiko, "Electrical control of the structure and lasing in chiral photonic band-gap liquid crystals," *Appl. Phys. Lett.* **82**, 16-18 (2003).
11. M. F. Moreira, I. C. S. Carvalho, W. Cao, C. Bailey, B. Taheri, and P. Palffy-Muhoray, "Cholesteric liquid-crystal laser as an optic fiber-based temperature sensor," *Appl. Phys. Lett.* **85**, 2691-2693 (2004).
12. Y. Huang, Y. Zhou, and S. T. Wu, "Spatially tunable laser emission in dye-doped photonic liquid crystals," *Appl. Phys. Lett.* **88**, 011107 (2006).
13. A. Chanishvili, G. Chilaya, G. Petriashvili, R. Barberi, R. Bartolino, G. Cipparrone, A. Mazzulla, and L. Oriol, "Phototunable lasing in dye-doped cholesteric liquid crystals," *Appl. Phys. Lett.* **83**, 5353-5355 (2003).
14. A. Y. G. Fuh, T. H. Lin, J. H. Liu, and F. C. Wu, "Lasing in chiral photonic liquid crystals and associated frequency tuning," *Opt. Express* **12**, 1857-1863 (2004).
15. Y. Zhou, Y. Huang, A. Rapaport, M. Bass, and S. T. Wu, "Doubling the optical efficiency of a chiral liquid crystal laser using a reflector," *Appl. Phys. Lett.* **87**, 231107 (2005).
16. Y. Zhou, Y. Huang, and S. T. Wu, "Enhancing cholesteric liquid crystal laser performance using a cholesteric reflector," *Opt. Express* **14**, 3906-3916 (2006).
K. Amemiya, T. Nagata, M. H. Song, Y. Takanishi, K. Ishikawa, S. Nishimura, T. Toyooka, and H. Takezoe, "Enhancement of laser emission intensity in dye-doped cholesteric liquid crystals with single-output window," *Jpn. J. Appl. Phys.* **44**, 3748-3750 (2005).

17. Q. Hong, T. X. Wu, and S. T. Wu, "Optical wave propagation in a cholesteric liquid crystal using the finite element method," *Liq. Cryst.* **30**, 367-375 (2003).
 18. E. Hecht, *Optics (2nd edition)*, Chapter 8, (Addison-Wesley, Massachusetts, 1987).
 19. P. G. de Gennes and J. Prost, *The Physics of Liquid Crystals (2nd edition)*, (Oxford University Press, New York, 1993).
 20. J. Li, G. Baird, Y. H. Lin, H. W. Ren, and S. T. Wu, "Refractive index matching between liquid crystals and photopolymers," *J. SID.* **13**, 1017-1026 (2005).
 21. K. Funamoto, M. Ozaki, and K. Yoshino, "Discontinuous shift of lasing wavelength with temperature in cholesteric liquid crystal," *Jpn. J. Appl. Phys.* **42**, L1523-L1525 (2003).
-

1. Introduction

Photonic crystals which exhibit an ordered structure with periodic dielectric constant in optical wavelength range have attracted tremendous attentions from both fundamental studies and practical applications. In such materials, the propagation of electromagnetic waves in a certain frequency range is prohibited and, therefore, photonic band gap (PBG) is established. Two-dimensional (2D) and three-dimensional (3D) photonic crystals show complete photonic band gap while one-dimensional (1D) photonic crystals do not. Even so, the strong localization of electromagnetic modes demonstrated in 1D photonic crystals within the photonic band gap or at the photonic band edge is especially useful for trapping the photons and shaping the density of states. Hence they are favorable for potential applications as low-threshold lasers, micro-waveguides, optical amplifiers, and other photonic devices.

Self-assembled with a periodic chiral structure, cholesteric liquid crystals (CLCs) can be regarded as 1D photonic crystals [1]. Compared to 2D and 3D devices, they present marked advantages on easy fabrication process, flexible manipulation, and good tuning capability. In their planar (Grandjean) structure, liquid crystal (LC) molecules are confined in the plane parallel to the substrates while rotate along the helical axis on a continuous basis. In this way, the PBG appears for the circularly polarized light. The circularly polarized light in the same handedness as the cholesteric helix is selectively reflected and the one in counter handedness is transmitted. The central wavelength (λ_0) and the bandwidth ($\Delta\lambda$) of PBG are determined by $\lambda_0 = p\langle n \rangle$ and $\Delta\lambda = p\Delta n$, where $\langle n \rangle$, Δn , and p represent the average refractive index, birefringence of the LC host, and intrinsic pitch length, respectively [2]. Because of the substantial decrease of group velocity and high density of states at photonic band edge, lasing action takes place when doped with active medium. The optical feedback can be provided through backward Bragg scattering, which is usually known as distributed feedback [3].

Based on this concept, extensive work has been conducted on the lasing action from cholesteric liquid crystals [4, 5] or other materials sharing a similar anisotropic chiral structure [6-9]. Wavelength tuning in these systems can be achieved by the control of chiral agent concentration, external electric field, temperature, photochemical effect and so on [10-14].

Because of chiral structure, laser emission generated from dye-doped CLCs is typically circularly polarized in the same sense as the cholesteric helix. Moreover, the symmetric structure leads to double-sided emission in the forward and backward directions, which is not considered very practical. In our previous work [15, 16], we demonstrated a single-sided laser extraction using a CLC reflector or a mirror reflector whereas the enhanced emission is still observed for the same circular polarization output. Similar work by Amemiya et al [17] using a spin-coated CLC film and evaporated aluminum layer inside LC cells was performed where only enhanced emission was reported with no discussion on the polarization states.

In this paper, we use an aluminum (Al) coated homogeneous cell to demonstrate a single-sided CLC laser and, moreover, the laser emission is dramatically enhanced due to double pumping effect. More importantly, the immediate contact between the active layer and the reflection layer enables coherent superposition of two orthogonal circular polarization states, which produces a *linearly* polarized laser beam with high linearity. Physical mechanisms are theoretically investigated, from which we understand that the rotation of the linear polarization direction can be well controlled by the temperature and the cell gap. Correspondingly, we demonstrated the rotation of linearly polarized laser beam using these

two methods. The experimental results are in good agreement with our theoretically predicted model. Such a method not only enhances the laser emission but also opens a way for flexible manipulation and control on the polarization state as well. Direction tunable linearly polarized laser devices would be useful for various photonic applications.

2. Sample preparation and experimental setup

In order to demonstrate the rotation period of linearly polarized laser, we made two different cholesteric liquid crystal mixtures with different birefringence. Mixture 1 is composed of high birefringence nematic liquid crystal BL006 ($\Delta n=0.28$, $n_e=1.81$ from Merck) and 27.3 wt% of right-handed chiral agent MLC6248 (twist power= $11.1\mu\text{m}^{-1}$, from Merck). Mixture 2 is composed of nematic liquid crystal ZLI-1694 ($\Delta n=0.13$, $n_e=1.62$ from Merck) and 22.9 wt% of MLC6248. Besides, 1-1.5 wt% of laser dye DCM (4-(dicyanomethylene)-2-methyl-6-(4-dimethylaminoethyl)-4H-pran, Exciton) was doped into the cholesteric liquid crystals as the active medium. The whole mixture was thoroughly mixed before it was capillary-filled into the homogeneous LC cell in an isotropic state. One of the inner surfaces was coated with aluminum as a mirror reflector and the other was coated with a thin indium-tin-oxide (ITO) transparent electrode. Polyimide layers were spun-coated on both sides and then rubbed in anti-parallel direction to produce 2-3° pretilt angle. After a slow cooling process, a defect-free single-domain cholesteric planar structure was formed.

For experimental setup, we used a reflective configuration at 30° oblique incidence. The pump source is a frequency-doubled Nd:YAG pulsed laser (Minilite II, Continuum) with pumping wavelength $\lambda=532$ nm, 4 ns pulse width, and 1 Hz repetition rate. The pump beam is separated into two paths with one of them monitored by the energy meter (Laserstar, Ophir) and the other focused on the CLC cell. Here, the circularly polarized pump in counter handedness with respect to the cholesteric helix is employed in order to reduce the CLC Bragg reflection even if the reflection band overlaps with the pump wavelength [18]. Then the emitted laser light is collected into fiber-based spectrometer (Ocean Optics, HR2000, resolution=0.4 nm) along the direction exactly perpendicular to the glass substrates where lies the periodic refractive index modulation.

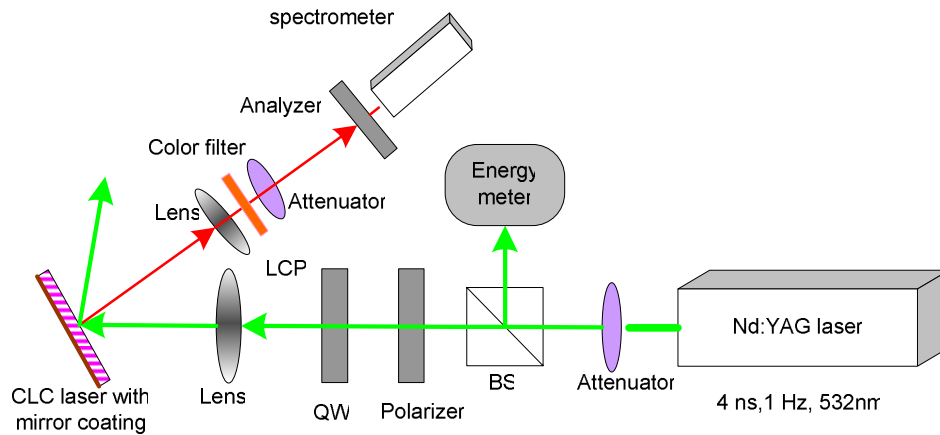


Fig. 1. Experimental setup at 30° oblique incidence. LCP: Left-handed circularly polarized light; QW: Quarter wave plate.

3. Theory of linearly polarized direction

Assuming wave propagates along +z axis, the electric field along x and y can be expressed as Eqs. (1)-(2) [19]:

$$\vec{E}_x = E_{x0} \cos(kz - \omega t), \quad (1)$$

$$\vec{E}_y = E_{y0} \cos(kz - \omega t + \delta), \quad (2)$$

where δ is the phase difference between \vec{E}_y and \vec{E}_x . For $\delta > 0$, \vec{E}_y lags behind \vec{E}_x by δ . Based on this convention, left-handed circularly polarized light (LCP) and right-handed circularly polarized light (RCP) can be denoted by Jones vector as $\frac{1}{\sqrt{2}} \begin{bmatrix} 1 \\ -i \end{bmatrix}$ and $\frac{1}{\sqrt{2}} \begin{bmatrix} 1 \\ i \end{bmatrix}$, respectively [20].

For a right-handed cholesteric liquid crystal, the original laser emitted from both sides is right-handed circularly polarized. Upon reflection at the mirror surface, the reflected laser beam gains a π phase change and thus becomes left-handed circularly polarized. Consequently, these two orthogonal laser beams would combine together based on coherent superposition, where LCP and RCP experience a different phase delay. The linear superposition of the two beams can be expressed as Eq. (3):

$$\begin{aligned} & \frac{1}{\sqrt{2}} \begin{bmatrix} 1 \\ i \end{bmatrix} + \frac{1}{\sqrt{2}} \begin{bmatrix} 1 \\ -i \end{bmatrix} e^{i\delta} \\ &= \frac{1}{\sqrt{2}} \begin{bmatrix} (1 + \cos \delta) + i \sin \delta \\ \sin \delta + i(1 - \cos \delta) \end{bmatrix} \\ &= \frac{1}{\sqrt{2}} \begin{bmatrix} (1 + \cos \delta) + i \sin \delta \\ \sin \delta + i(1 - \cos \delta) \end{bmatrix} \times \begin{bmatrix} (1 + \cos \delta) - i \sin \delta \\ (1 + \cos \delta) - i \sin \delta \end{bmatrix} \\ &= \sqrt{2} \begin{bmatrix} 1 + \cos \delta \\ \sin \delta \end{bmatrix} \\ &\propto \begin{bmatrix} \cos(\delta/2) \\ \sin(\delta/2) \end{bmatrix} \end{aligned} \quad (3)$$

where $\delta = 2\pi OPD/\lambda$ is the phase delay between LCP and RCP, and OPD represents the optical path difference. When the two circularly polarized beams combine together including a phase delay between them, it gives out a linearly polarized light oriented along the $\delta/2$ direction.

Because of periodic index modulation, the cholesteric liquid crystal builds up a good Bragg reflection (with reflectivity higher than ~98%) as long as the number of pitches is above 15 [18]. RCP and LCP are two orthogonal eigen-modes. Given a right-handed CLC, within the reflection band, RCP experiences high reflectivity while LCP directly transmits through. Therefore, we can infer that RCP sees the refractive index modulation as $n_e-n_o-n_e-n_o\dots$ when propagating through the medium while LCP sees an isotropic medium with refractive index n_o . On the other hand, the original laser generated from different layers of CLC is assumed to be completely in phase because the time duration for the laser passing through the distance of a cell gap (only few microns) is so much smaller than the pulse duration (ns) of the pumping beam. Furthermore, each periodic medium (i.e. each pitch) produces a 2π reflective phase shift. Thus, the reflection after multiple pitches is constructive with zero phase shift.

Consequently the accumulation of phase delay δ over the periodic medium can be described as:

$$\delta = \frac{2\delta}{\lambda_0} OPD = \frac{2\delta}{\lambda_0} \cdot \frac{\Delta n_{eff} d}{2} \quad (4)$$

Let λ_0 , d and $\Delta n_{eff} = \Delta n \cdot c$ wt% be the lasing wavelength, cell gap, and the effective birefringence of the cholesteric mixture, respectively. Δn and c wt% are the birefringence and weight concentration of the nematic liquid crystal.

From Eqs. (3)-(4), it is seen that a decrease in cell gap d causes a smaller phase delay and the decrease of the linear polarization angle ensues. In other words, when facing the laser propagation direction, we expect to observe the linearly polarized light rotating clockwise.

4. Experimental results

4.1. Enhanced linearly polarized laser emission

Figure 2 plots the transmission spectrum of normal dye-doped CLC lasers without mirror coating. Two samples, made of CLC mixture 1 (using BL006) and 2 (using ZLI-1694), are shown in blue and green, respectively. The data for CLC samples without DCM dopant give an 80 nm reflection band width for BL006 mixture and 40 nm for ZLI 1694 mixture (not shown here). The shorter wavelength edge of the reflection band is somewhat obscured depending on different dye concentrations. As an example, the lasing spectrum from mirror reflective CLC laser using BL006 mixture is plotted as well. The lasing wavelength is 601 nm for the BL006 CLC laser and 610 nm for the ZLI-1694 CLC laser. The FWHM of laser line is around 0.8 nm.

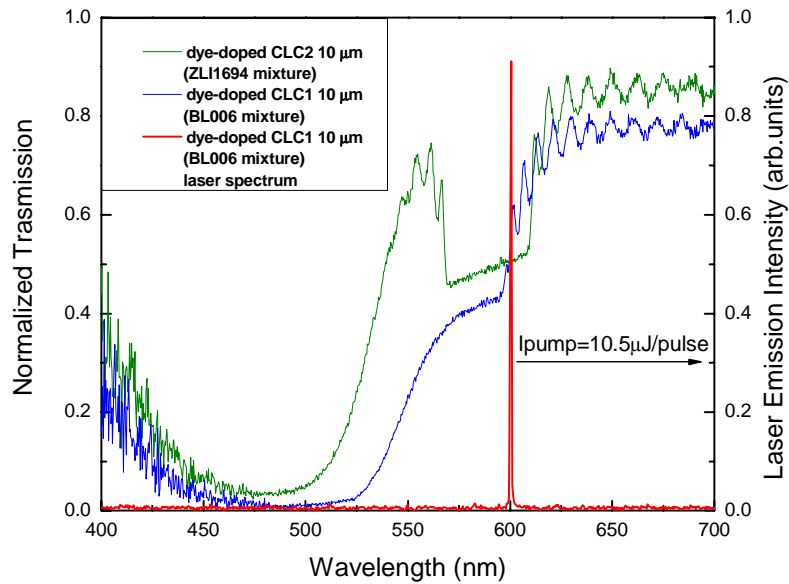


Fig. 2. Reflection spectra of a 10- μ m-thick dye-doped CLC sample 1 (BL006 +27.3% MLC6248 + 1.5% DCM), a 10- μ m-thick CLC sample 2 (ZLI1694+22.9% MLC6248+1% DCM), and lasing spectrum from mirror reflective CLC laser using mixture 1.

Using the setup shown in Fig. 1, we measured the laser emission from the dye-doped BL006 CLC sample in a 10 μm cell with mirror coating on one substrate. Figures 3(a)-3(b) depict the laser output power change along different analyzer direction at pumping energy of 30 $\mu\text{J}/\text{pulse}$ and 10 $\mu\text{J}/\text{pulse}$. The blue line shows the experimental results and the red line shows the simulation results, calculated according to Malus's Law [19] as Eq. (5) shows:

$$I_{\text{output}} = \cos^2(\phi) \quad (5)$$

Here I_{output} is the output power after the analyzer and ϕ is the relative angle between the linearly polarization direction and the analyzer. Results here indicate that when rotating the analyzer before the detector, we observed the laser emission power changes as square of cosine at both low and high pumping energies.

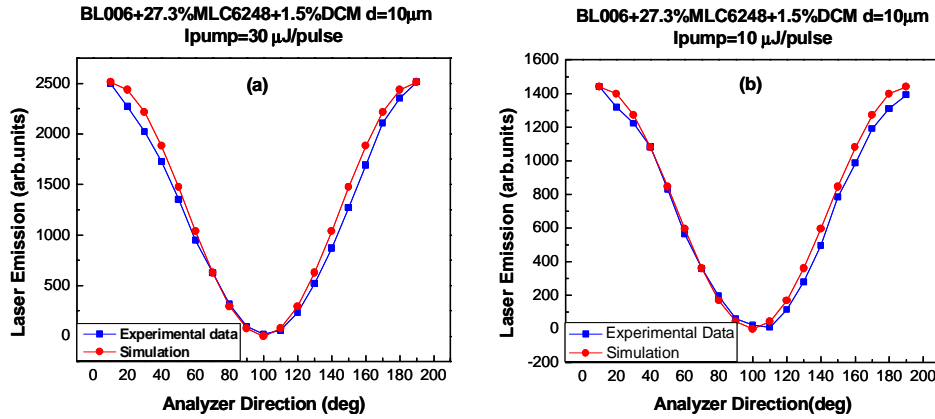


Fig. 3. Linearly polarized laser output power change with the analyzer direction. (a): pump energy at 30 $\mu\text{J}/\text{pulse}$ and (b): pump energy at 10 $\mu\text{J}/\text{pulse}$.

To evaluate the purity of the linearly polarized light, we define the linearity β as:

$$\beta = \frac{I_{\text{max}} - I_{\text{min}}}{I_{\text{max}} + I_{\text{min}}}, \quad (6)$$

where I_{max} and I_{min} represent the maximum and minimum light intensity when rotating the analyzer. A perfect linearly polarized light gives $\beta=1$. Under this definition, our measured data show a linearity $\beta=0.986$ at both high and low pump, indicating a very pure linearly polarized laser light.

In comparison, we also measured the output power from a normal CLC sample and the CLC sample with mirror coating. Figure 4 shows the pump energy dependent laser emission with red line representing the CLC laser with mirror coating and blue line representing the normal CLC laser. The threshold energy was measured to be 0.7 $\mu\text{J}/\text{pulse}$ and 1.2 $\mu\text{J}/\text{pulse}$, respectively. It is found that the mirror reflective CLC has a stronger laser emission than the normal one under the same setup configuration. Although the normal CLC laser emits photons from both sides rather than single side as the mirror reflective CLC laser does, the average enhancement ratio (the output ratio between these two lasers) reaches $\sim 5.6\text{X}$, much higher than twice. That means the mirror reflective CLC laser has much higher efficiency, which is attributed to the double pump during the path of laser generation. In our experiment, the pump beam is around $\sim 200\mu\text{m}$ in diameter. Hence for the 10 μm cell gap, the pump beam can be almost completely reflected back to the original pumping area even at an oblique incidence.

In this section, we have demonstrated that the mirror reflective CLC laser generates very pure linearly polarized laser light and, furthermore, such a reflective structure substantially enhances the laser output compared to the normal CLC laser. In the meantime, we also found that the orientation of the linearly polarized laser light exactly followed the rotation of the whole cell. This fact implies the linear polarization direction is associated with the LC cell's rubbing direction. Though the cholesteric liquid crystal has a symmetric structure, the rubbing direction determines the boundary conditions, which accounts for the reference axis of the linear polarization direction.

In the following section, we discuss the control of linear polarization direction by means of temperature and cell gap.

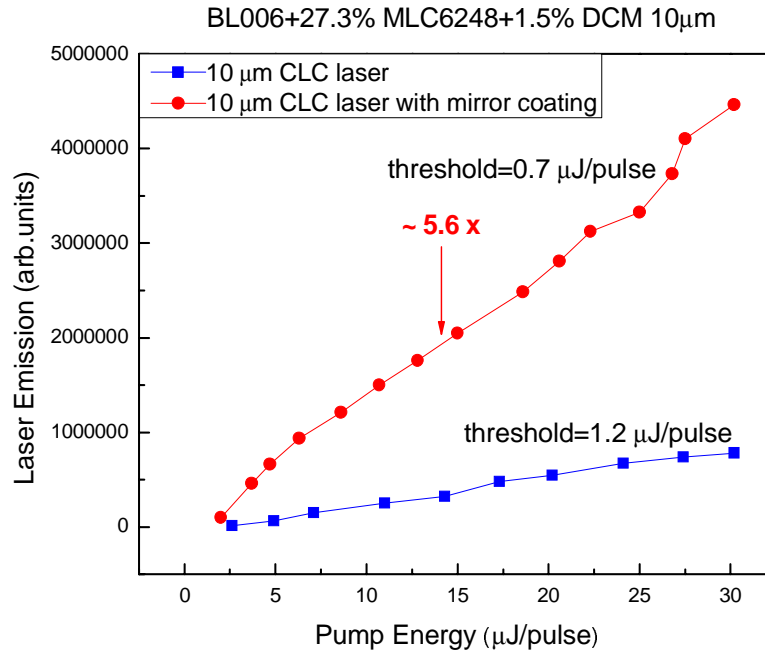


Fig. 4. Pumping energy dependent laser emission from a 10-µm normal CLC laser and a mirror reflective CLC laser.

4.2. Rotating linearly polarized laser light direction with temperature

From Eq. (4), we know that the phase delay between two eigen modes, RCP and LCP are determined by lasing wavelength and effective birefringence, both of which are temperature sensitive. Therefore, we positioned the mirror reflective CLC laser (the same sample as used in Sec. 4.1) on a temperature controller so that we observed the linear polarization rotated with the temperature change. Meanwhile, we used Eq. (4) to calculate the theoretical value of linear polarization rotation according to the exact effective birefringence at a specific lasing wavelength and temperature. Both measured data and theoretical calculation are listed in Table 1. The refractive index of BL006 at different temperatures and lasing wavelengths are extracted from the fitting curve, whose original data are measured using Abbe Refractometer (Atago DR-M4) and standard color filters [21].

Figure 5 describes both theoretical and measured data of linear polarization direction rotation with the increase of temperature. Here the direction angle is normalized to the end direction at 55 °C. The experimental results match very well with the theoretical calculation.

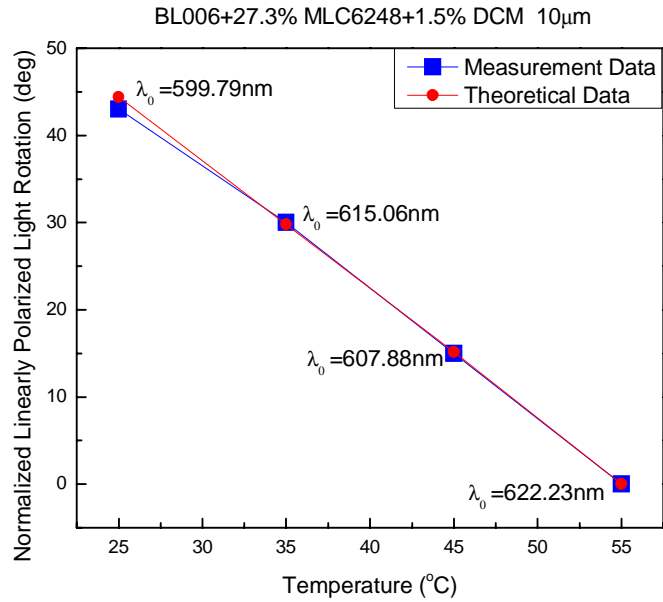


Fig. 5. Temperature dependent normalized linearly polarized light direction.

Table 1. Calculated and measured linear polarization direction rotation at different temperatures.

| | 25°C | 35°C | 45°C | 55°C |
|--|--------|--------|--------|--------|
| λ_0 (nm) | 599.79 | 607.88 | 615.06 | 622.23 |
| n_e | 1.8067 | 1.7943 | 1.7813 | 1.7682 |
| n_o | 1.5275 | 1.5249 | 1.5225 | 1.5208 |
| Δn | 0.2792 | 0.2694 | 0.2588 | 0.2474 |
| $\Delta n_{\text{eff}} = \Delta n \cdot c \%$ | 0.2030 | 0.1959 | 0.1882 | 0.1799 |
| $\delta = \frac{2\pi}{\lambda_0} \cdot \frac{\Delta n d}{2}$ (rad) | 10.63 | 10.12 | 9.61 | 9.08 |
| $\theta_{\text{calculated}} = \delta/2$ (deg) | 44.4 | 29.8 | 15.1 | 0 |
| θ_{measured} (deg) | 43.0 | 30.0 | 15.0 | 0 |

4.3. Rotating linearly polarized laser light direction using a wedged cell

Results presented above demonstrate that linear polarization direction can be tuned by controlling the temperature. However, as reported in Ref. [22], lasing wavelength shifts

discontinuously with temperature, and thus a discontinuous tuning of polarization direction. In order to fine tune the direction in a continuous manner, we made a wedged cell with cell gap varied around $\sim 8\text{-}15\ \mu\text{m}$. Because the cell gap increases gradually in a row within a wedged cell, polarization direction can be controlled continuously.

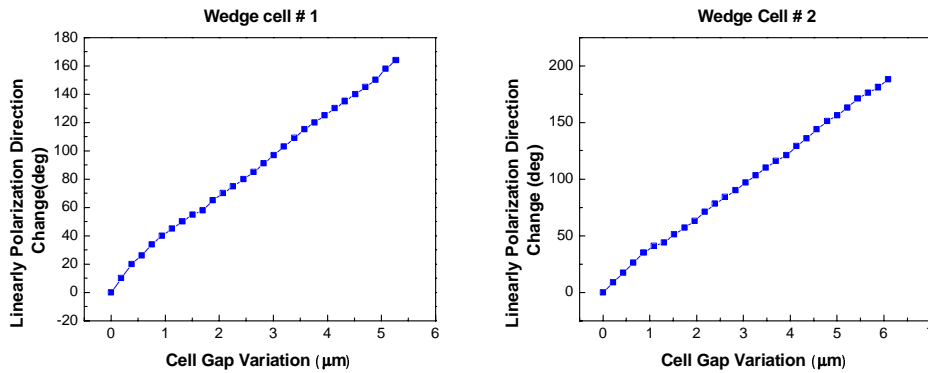


Fig. 6. Cell gap variation dependent linear polarized light rotation for wedge cell #1(left) and wedge cell #2 (right) by mixture 1 (BL006 + 27.3%MLC6248 + 1.5%DCM).

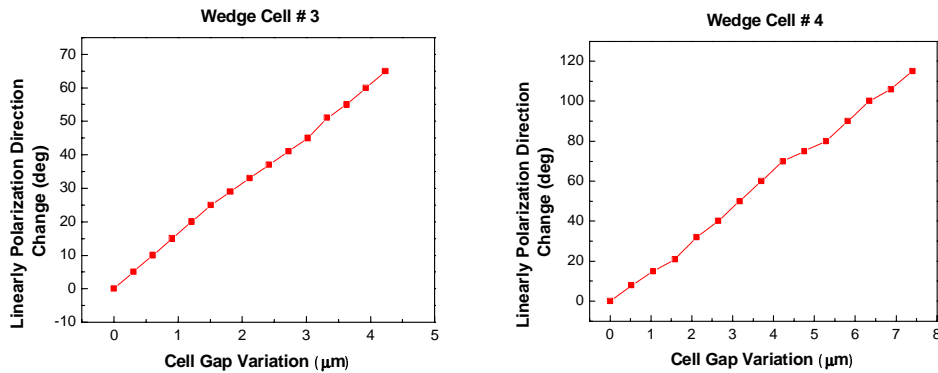


Fig. 7. Cell gap variation dependent linear polarized light rotation for wedge cell #3(left) and wedge cell #4 (right) by mixture 2 (ZLI1694 + 22.9%MLC6248 + 1 %DCM).

Using the CLC mixture 1 (BL006+27.3%MLC6248+1.5%DCM), we made two different wedged CLC lasers with a relatively large birefringence. Using CLC mixture 2 (ZLI6248 +22.9%MLC6248+1%DCM) we made the other two wedged CLC lasers with birefringence almost half of the first one. Subsequently CLC laser is scanning-pumped across the fringes. At different scanning positions, linear polarization direction is measured to rotate linearly with the cell gap variation, as shown in Fig. 6 (wedged cells #1 and #2, from CLC mixture 1) and Fig. 7 (wedged cells #3 and #4, from CLC mixture 2). According to the rotation angle over the measured cell gap variation, the rotation period, which means the thickness variation over which the linearly polarized light will rotate 180° , can be obtained. In these figures, polarization direction angle is normalized to the starting point on the thinner side of the wedged cell. Due to the birefringence difference, the wedged cells #3 and #4 exhibit almost twice of rotation period as the wedged cells #1 and #2. Detailed calculation results are listed in Table 2. The theoretically calculated rotation period $P_{\text{calculated}}$ matches well with the experimental rotation period p_{measured} , where the error is within 1-2 fringes.

Table 2. Calculated and measured linear polarization rotation period for mixture 1 (BL006+27.3%MLC6248 +1.5%DCM) and mixture 2 (ZLI-6248+22.9%MLC6248+1%DCM). $P_{calculated}$ and $P_{measured}$ are calculated rotation period and measured rotation period. N is the number of fringes and d is the cell gap variation over the measured range. λ_{VIS} is chosen as 550 nm, the center of visible light.

| | BL006+27.3%MLC6248 +1.5% DCM | | ZLI1694 + 22.9%MLC6248 + 1.5% DCM | |
|---|---|-----------------|--|-----------------|
| $\langle n \rangle$ | 1.67 | | 1.56 | |
| Δn | 0.28 | | 0.13 | |
| $\Delta \lambda$ (nm) | 80 | | 40 | |
| $\Delta n_{eff} = \Delta n \cdot c\%$ | 0.204 | | 0.102 | |
| $P_{calculated} = \frac{2 \cdot \lambda_0}{\Delta n_{eff}}$ (μm) | 5.8 | | 11.9 | |
| | Wedge #1 | Wedge #2 | Wedge #3 | Wedge #4 |
| N (# of fringes) | 32 | 37 | 24 | 42 |
| $d = \frac{\lambda_{VIS} \cdot N}{2 \cdot \langle n \rangle}$ (μm) | 5.27 | 6.09 | 4.23 | 7.4 |
| $\Delta \theta$ (deg) | 164 | 188 | 65 | 115 |
| $P_{measured} = \frac{d \cdot 180^\circ}{\Delta \theta}$ (μm) | 5.78 | 5.83 | 11.72 | 11.59 |

5. Conclusion

We have demonstrated linearly polarized lasers from dye-doped cholesteric liquid crystals with an aluminum mirror coated on an inner surface of a glass substrate. The enhanced linearly polarized light shows very good linearity. Moreover, the rotation effect is theoretically analyzed and then experimentally validated. Based on this effect we used the temperature and cell gap to control the linear polarization direction and realized the direction tunable CLC laser devices. Such a device is highly useful for the polarization manipulation.

Acknowledgment

The authors are indebted to Prof. Patrick LiKamWa from CREOL, University of Central Florida for stimulating discussion and Dr. Xinyu Zhu from CREOL, University of Central Florida for great support on liquid crystal cells.